Progress In Electromagnetics Research Letters, Vol. 66, 127–134, 2017

The Testing Scheme for Steel Corrosion in the Reinforced Concrete via Near Field Effect of Meter-Band Wave

Ruiqiang Zhao[1], Hong Zhang[2], Jianting Zhou[2], Leng Liao[1, *], and Runchuan Xia[2]

Abstract—This paper presents a testing scheme for the steel corrosion in reinforced concrete based on near-field effect of meter wave. The physical mechanism of the near-field method was introduced, and the structure of the measurement device was presented in detail. The electromagnetic field near the steel bar buried in the concrete structure was simulated by the finite difference time domain method. The simulated data show that the mean radiation power decreases monotonously with the increase of the corroded depth of the steel bar, and the corroded area is promising to be imaged directly due to the localization of near field. The results indicate that the near-field technique can act as a new nondestructive testing technique to detect and even image the corrosion area buried in concrete in engineering structure.

1. INTRODUCTION

Reinforced concrete (RC) is the most popular construction material in the world due to the advantage of strong bearing, low cost, and easy construction. However, a degradation issue for RC structures is the corrosion of interior steel bar. It makes a significant contribution to the failure of engineering structure. Roughly 40% of the engineering structure damages result from the steel corrosion [1]. Many techniques have been developed to detect and evaluate the steel failures [2], such as electrochemical method [3, 4], linear ultrasonic testing (UT) [5], acoustic emission (AE) [6–8], eddy current testing (ECT) [9–11], infrared thermography (IRT) [12–14], ground penetrating radar (GPR) [15], magnetic flux leakage (MFL) [16, 17], electronic resistance testing (ERT) [18], fiber bragg grating (FBG) [19, 20], and X-ray diffraction (XRD) [21]. However, in the field of identification of corrosion in the steel components in RC structure, nondestructive test (NDT) is the optimal selection, because the mechanical integrity of RC structure is always required after inspection. For this reason, electromagnetic (EM) methods play important roles in the evaluation of RC structures, and many EM methods, such as ECT [9–11], MFL [16, 17], GPR [15], have been developed. ECT method uses a coil of conductive wire excited with an alternating electrical current to produce an alternating magnetic field. When the coil approaches a conductive material, currents opposed to the ones in the coil are induced in the material (called eddy currents). The presence of defects causes a change in eddy current, and a corresponding change in phase and amplitude that can be detected to evaluate the defects. The basic principle of MFL is that a powerful magnet is used to magnetize the steel. At areas where there is corrosion or missing metal, the magnetic field "leaks" from the steel. In an MFL tool, a magnetic detector is placed between the poles of the magnet to detect the leakage field. Analysts interpret the chart recording of the leakage field to identify damaged areas and to estimate the depth of metal loss. GPR uses high-frequency EM waves, usually in the range from 10 MHz to 2.6 GHz. A GPR transmitter emits electromagnetic energy into the ground. When the energy encounters a buried object or a boundary between materials having different

Received 14 January 2017, Accepted 22 February 2017, Scheduled 13 March 2017

* Corresponding author: Leng Liao (lengliao@cqjtu.edu.cn).

[1] School of Materials Science and Engineering, Chongqing Jiaotong University, Chongqing 400074, China. [2] College of Civil Engineering, Chongqing Jiaotong University, Chongqing 400074, China.

permittivities, it may be reflected or refracted or scattered back to the surface. A receiving antenna can then record the variations in the return signal. Nevertheless, these conventional EM methods still have some disadvantages to the test of steel corrosion in RC structures. Because of the thick concrete cover on the steel components, for the low frequency methods (ECT, MFL), the EM exciting needs much stronger intensity than that in the test of bare components, and it makes the exciting equipment very heavy. On the other hand, for the high frequency methods, for example, the GPR by the microwave, the absorption and scattering of EM wave in the concrete are very strong, and thus the acquired signals are very complicated for the latter analysis, which needs sophisticated instruments and makes the test systems very expensive.

In present work, we propose a simple, lightweight and cheap method to test steel corrosion in the RC structures via the near-field effect of meter-band EM wave. Both the near field (NF) and far field (FF) are the electromagnetic field around the antenna or the result of radiation scattering off an object [22–24]. The FF acts as the 'normal' EM radiation, while the NF is non-radiative [25]. In contrast to the FF, the intensity of the NF decreases rapidly with the increase of the distance from the antenna; therefore, the NF just acts close to the antenna or the scattering objects ($r \ll \lambda$), but the strength of NF is much stronger than the FF in the close range ($r \ll \lambda$). More importantly, the NF does not obey the Rayleigh criterion [26] and can deliver the sub-wavelength information of the scattering or reflecting objects [27, 28]. For this reason, the NF method has been widely used in microscope and achieved great success in the nanotechnology in recent years [29, 30].

Up to now, the NF techniques are mainly focused on the characterization of micro-structure, and the EM waves adopted are mainly short-wavelength EM waves such as light or microwave [25, 26]. In present work, we apply the NF method on the non-destructive test of macro-structure and propose a scheme to test and even image the steel corrosion under concrete by analyzing the diffracted NF of meter-band wave ($\lambda \sim 0.5\,\mathrm{m}$), because meter-band wave can effectively penetrate the concrete cover and has a long active NF distance for the long-wavelength. It is a simple, lightweight and cheap method to evaluate the failure of steel locating in the subsurface of RC structure.

The paper is organized as follows. In Section 2, the test model by NF is proposed, and the related electromagnetic theory is discussed. In Section 3, the calculated results by using the finite difference time domain (FDTD) method are presented to verify the feasibility of this testing scheme for the steel corrosion buried in RC. In Section 4, we summarize all these results.

2. NEAR FIELD THEORY AND TESTING MODEL

For simplicity, we first begin with a simple system, which is the electric dipole oscillator, to interpret the NF around an object. If only considering the first order approximation, the vector potential generated by a current distribution is expressed in frequency domain as [30, 31]

$$\mathbf{A}(\mathbf{x},\omega) = \frac{\mu_0}{4\pi}\frac{e^{ikr}}{r}\int \mathbf{J}(\mathbf{x}',\omega)d^3\mathbf{x}', \tag{1}$$

where $\mathbf{A}(\mathbf{x},\omega)$ is the vector potential; $\mathbf{J}(\mathbf{x}',\omega)$ is the current density; k and ω are wave vector and angular frequency, respectively, which satisfy the dispersion relation: $c^2k^2 = \omega^2$; r is the distance between electric dipole and the observing point $\mathbf{x}$; μ_0 is the permeability of vacuum.

The integral in Equation (1) can be put in terms as

$$\int \mathbf{J}(\mathbf{x}',\omega)d^3\mathbf{x}' = -\int \mathbf{x}'(\boldsymbol{\nabla}'\cdot\mathbf{J})d^3\mathbf{x}' = -i\omega\int \mathbf{x}'\rho(\mathbf{x}',\omega)d^3\mathbf{x}', \tag{2}$$

since the continuity equation

$$i\omega\rho(\mathbf{x},\omega) = \boldsymbol{\nabla}\cdot\mathbf{J}(\mathbf{x},\omega), \tag{3}$$

where $\rho(\mathbf{x},\omega)$ is the charge distribution in frequency domain. Thus the vector potential for an electric dipole oscillator is

$$\mathbf{A}(\mathbf{x},\omega) = -\frac{\mathrm{i}\mu_0\omega}{4\pi}\frac{e^{-ikr}}{r}\mathbf{p}(\omega), \tag{4}$$

where

$$\mathbf{p}(\omega) = \int \mathbf{x}'\rho(\mathbf{x}',\omega)d^3\mathbf{x}' \tag{5}$$

is the electric dipole moment. By the equations

$$\mathbf{H}(\mathbf{x},\omega) = \frac{1}{\mu_0}\boldsymbol{\nabla}\times\mathbf{A}(\mathbf{x},\omega) \tag{6}$$

$$\mathbf{E}(\mathbf{x},\omega) = \frac{i\sqrt{\mu_0/\varepsilon_0}}{k}\boldsymbol{\nabla}\times\mathbf{H}(\mathbf{x},\omega), \tag{7}$$

the magnetic intensity $\mathbf{H}(\mathbf{x},\omega)$ and electric intensity $\mathbf{E}(\mathbf{x},\omega)$ of the electric dipole are given as

$$\begin{aligned}\mathbf{H}(\mathbf{x},\omega) &= \frac{ck^2}{4\pi}(\mathbf{n}\times\mathbf{p})\frac{e^{ikr}}{r}\left(1-\frac{1}{ikr}\right)\\ \mathbf{E}(\mathbf{x},\omega) &= \frac{1}{4\pi\varepsilon_0}\left\{\frac{k^2e^{ikr}}{r}\left[(\mathbf{n}\times\mathbf{p})\times\mathbf{n}\right]+\left[3\mathbf{n}(\mathbf{n}\cdot\mathbf{p})-\mathbf{p}\right]\left(\frac{1}{r^3}-\frac{ik}{r^2}\right)e^{ikr}\right\}\end{aligned}, \tag{8}$$

where $\mathbf{n}$ is the unit vector from the electric dipole to the observing point. In the far zone where $kr \gg 1$ or $r \gg \lambda$, the field takes on the limiting forms

$$\begin{aligned}\mathbf{H}(\mathbf{x},\omega) &= \frac{ck^2}{4\pi}(\mathbf{n}\times\mathbf{p})\frac{e^{ikr}}{r}\\ \mathbf{E}(\mathbf{x},\omega) &= \sqrt{\mu_0/\varepsilon_0}\mathbf{H}\times\mathbf{n}\end{aligned}, \tag{9}$$

showing the typical behavior of radiation fields (far field), while in the near zone where $kr \ll 1$, or $r \ll \lambda$, the fields approach

$$\begin{aligned}\mathbf{H}(\mathbf{x},\omega) &= \frac{ick}{4\pi}(\mathbf{n}\times\mathbf{p})\frac{e^{ikr}}{r^2}\\ \mathbf{E}(\mathbf{x},\omega) &= \frac{1}{4\pi\varepsilon_0}\left[3\mathbf{n}(\mathbf{n}\cdot\mathbf{p})-\mathbf{p}\right]\frac{e^{ikr}}{r^3}\end{aligned}, \tag{10}$$

showing behavior of NF near the electric diploe oscillator. From Equation (10), we can note that the NF decays with r^2 or r^3, while the FF of Equation (9) attenuates with r^1; therefore, the NF is non-radiative and just acts in the near zone ($r \ll \lambda$). By the same token, the NF is accordingly much stronger than the FF where $r \ll \lambda$; therefore, the NF is sensitive to the distance from the antenna and has a stronger power in the near zone. Using NF wave to irradiate the failure of conductive structures, more sensitive feedback can be obtained. Moreover, NF wave is a local effect in the near zone $r \ll \lambda$, which means that the NF signals have much better anti-interference ability than the FF signals and can acquire sub-wavelength information. For this reason, NF effect has been broadly applied to the new generation of optical microscopy (near field optical microscope (NFOM)) [29, 30].

Based on the theory mentioned above, we propose a testing scheme for steel corrosion via NF of meter wave as sketched in Figure 1. Similar to the NFOM system, it is mainly composed of a waveguide with a conical tip and a power meter to measure radiation power. However, the adopted wave source is not the light as NFOM, but the meter-band radio wave. There is a narrow slit on the cone tip, whose width is far shorter than the wavelength of the irradiated meter wave. TM meter wave is irradiated on the slits along the waveguide, and there will be diffraction wave generated at the other side of the slit. Because of the slit width shorter than the wavelength, the diffraction can be regarded as a radiation from an effective electric dipole oscillator in the slit [9], and the diffraction field is also composed of both the NF and the FF expressed in Equation (8). If a conductive object lies in the near zone of the slit, there will be field coupling between the cone tip and the object, and a reflected NF will be produced near the surface of the conductive object. When the reflected NF interacts with the cone tip, by the reciprocity between the NF and FF, the NF wave will be scattered, and a reemitted radiation is generated near the cone tip, which is called near/far field transformation by a small limited object [30, 32]. The power of this reemitted radiation can reflect the degree of EM coupling between the cone tip and the object. A radio frequency (RF) power meter is installed to measure this reemitted radiation in the far zone from the tip. If there is a corroded area in the object, the distance between the tip and the conductive body will increase, and the reflection of NF is consequently decreased because the NF will rapidly decay by the distance from the reflecting object. As a result, the reemitted radiation power is weakened. By measuring the power of the reemitted radiation at different positions, we can evaluate the corrosion status of steel bars buried in the concrete [33].

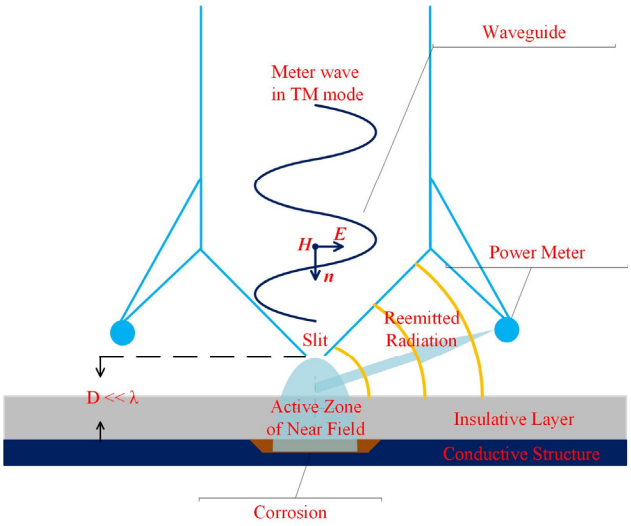

Figure 1. The schematic of test system by NF of meter wave.

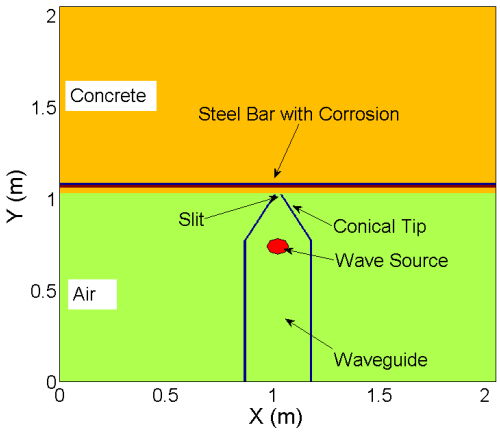

Figure 2. The schematic of simulation model.

3. NUMERICAL SIMULATION RESULTS

To verify the feasibility of this scheme for corrosion testing in RC structure, the numerical simulation is carried out by the finite difference time domain (FDTD) method, which is a popular numerical algorithm for electromagnetic simulation. The simulations were carried out in a domain of 2 m by 2 m represented by a 2048×2048 grids, and the perfectly matched layer (PML) is taken at the boundaries of the box to absorb boundary reflection. The waveguide and conical tip were modeled as shown in Figure 2. The width of the waveguide is 0.25 m, and the width of the slit on the conical tip is 2.5 cm, which is far shorter than the wavelength taken in simulation (λ is chosen to be 0.5 m). An EM field source is placed in the waveguide to excite the meter wave of EM mode. A RC structure with one steel bar is placed under the conical tip. The distance from the conical tip to the structure surface is 0.5 cm. The concrete thickness is chosen as 3 cm (a typical thickness for engineering structure).

The meter wave is excited in the waveguide and propagates to the conical tip. Because the slit width is much shorter than the wavelength, a strong NF wave is generated near the tip, which can penetrate the concrete cover. As discussed in Section 2, the NF reflected from steel bar will interact with the conical tip and produce the reemitted radiation by the near/far field transformation. If the corrosion occur on the steel surface, the distance between the tip and the steel bar will increase, and the reflected NF reaching the tip will be weakened. As a result, the reemitted radiation from the tip is weakened. The calculated EM field distributions for a healthy steel bar and a corroded bar (corrosion depth $d = 2.0$ cm) are shown in Figure 3. As shown in the above discussion, the reemitted radiation for the corroded bar is indeed weakened in comparison with the healthy steel bar.

Furthermore, we define the amplitude of the EM oscillation as

$$\mathbf{B}(\mathbf{x}) = \sqrt{\frac{\int_0^t \mathbf{B}(\mathbf{x}, t')^2 dt'}{t}}, \tag{11}$$

which represents the average field strength, and Figure 4 shows the calculated amplitudes of the EM oscillation for the corroded and the healthy bars. There exist strong fields around both the steel bar and the conical tip for either the healthy bar or the corroded bar. However, the fields around the steel bar and conical tip combine in the healthy case, while these fields are apart from each other in the corroded case. The difference implies that steel corrosion weakens the interaction of NF between the steel bar and the tip. The distance between the conical tip and the reflector is increased for the corrosion. The

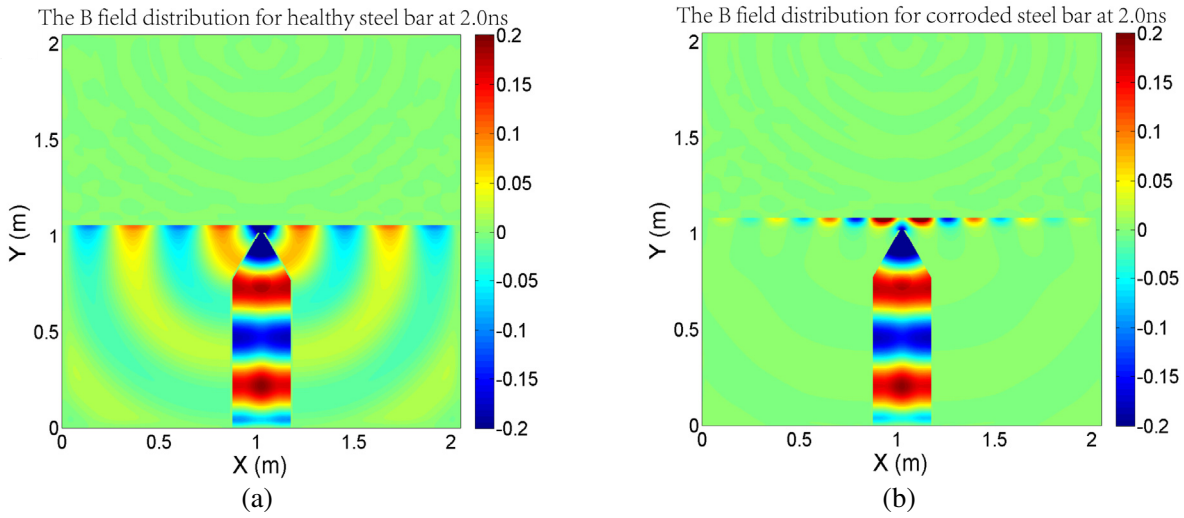

Figure 3. (a) The B field (wave field) distribution for a healthy steel bar; (b) the B field (wave field) distribution for a corroded steel bar.

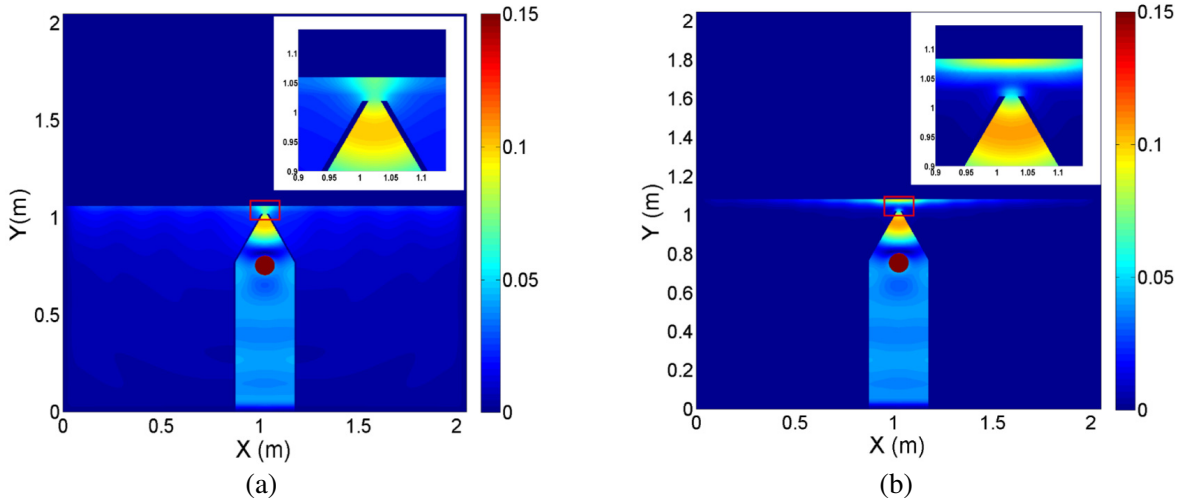

Figure 4. The amplitude distribution of the EM oscillation (a) for healthy steel bar and (b) for corroded steel bar.

NF wave reflected from steel needs to propagate over a longer distance to reach the conical tip. As a result, the reemitted wave excited by reflected NF is weakened because the NF wave decays quickly with the increase of propagation distance as expressed in Equation (10).

To give a further investigation on the relation between the reemitted wave and the steel corrosion, the reemitted radiation power dependence on the increase of the corrosion depth is calculated by the FDTD method. The calculated results are plotted in Figure 5, where the instantaneous radiation powers for different corrosions are shown in Figure 5(a), and the mean radiation power dependence on the corrosion depth is shown in Figure 5(b). The reemitted radiation power is monotonically decreased with the increase of the corrosion depth. It indicates that the reemitted radiation power can reflect the corrosion level. Furthermore, because of the localization of NF, we can directly obtain the detailed "image" of the steel structure buried in the concrete by moving the conical tip to scan the whole plane similar to the procedure in the optical NF microscope.

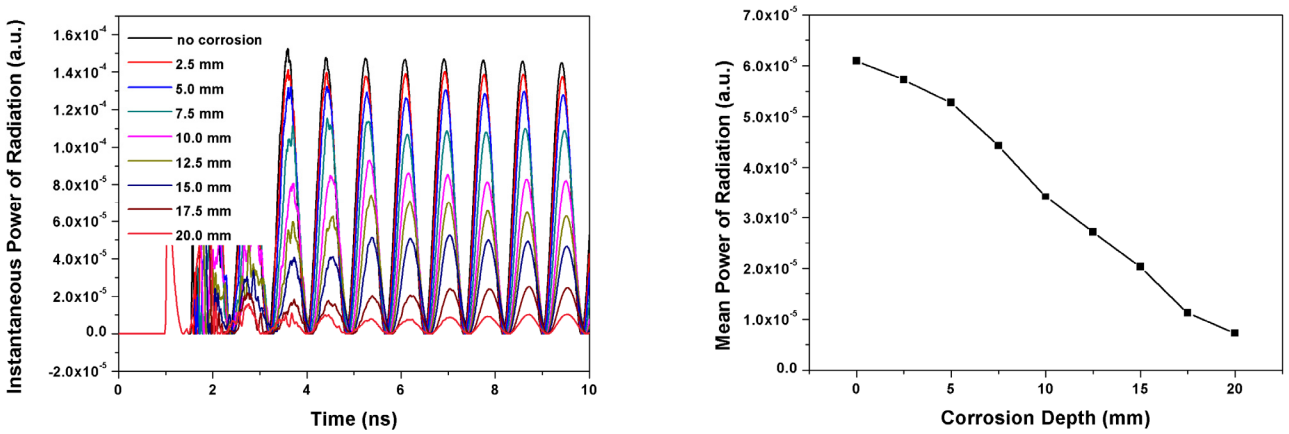

Figure 5. (a) The instantaneous power of reemitted radiation from the tip for different corrosion levels; (b) the mean radiation power for the different corrosion depth.

4. CONCLUSIONS

In conclusion, we proposed a testing scheme for the steel corrosion failure in reinforced concrete structure by detecting the reflected NF generated by steel object. The relevant NF theory was discussed by an electric dipole oscillator model. Furthermore, the specific electromagnetic processes for this testing scheme were simulated by the FDTD method. Based on the calculated results, we analyzed the working mechanism and verified the feasibility of the testing scheme. The results mean a new NDT technique to detect and even image the inner corrosion area in engineering structures.

ACKNOWLEDGMENT

This work was supported by the National Science Fund for Distinguished Young Scholars of China (No. 51425801), the National Key Research and Development Program of China (No. 2016YFC0802202), the National Natural Science Foundation of China (Nos. 11404045, 51508058, 51278512), the Chinese Academy of Engineering Consulting Project (Nos. 2015-XZ-28, 2016-XY-22), the Social Livelihood Science and Technology Innovation Special of Chongqing (No. cstc2015shmszx30012), the Science and Technology Project of Yunnan Provincial Transportation Department (No. 2014 (A) 27), and the Communications Science and Technology Project of Guangxi Province of China (No. 20144805).

Original Contribution

A testing scheme for the steel corrosion in reinforced concrete based on near-field effect of meter wave was proposed. The electromagnetic field near the steel bar buried in the concrete structure was simulated by the finite difference time domain method.

REFERENCES

1. Zhu, X., G. Zi, W. Lee, S. Kim, and J. Kong, "Probabilistic analysis of reinforcement corrosion due to the combined action of carbonation and chloride ingress in concrete," *Constr. Build. Mater.*, Vol. 124, 667–680, 2016.
2. Rehman, S. K. U., Z. Ibrahim, S. A. Memon, and M. Jameel, "Nondestructive test methods for concrete bridges: A review," *Constr. Build. Mater.*, Vol. 107, 58–86, 2016.
3. Česen, A., T. Kosec, and A. Legat, "Characterization of steel corrosion in mortar by various electrochemical and physical techniques," *Corros. Sci.*, Vol. 75, 47–57, 2013.

4. Reou, J. S. and K. Y. Ann, "Electrochemical assessment on the corrosion risk of steel embedment in OPC concrete depending on the corrosion detection techniques," *Mater. Chem. Phys.*, Vol. 113, No. 1, 78–84, 2009.
5. Yeih, W. and R. Huang, "Detection of the corrosion damage in reinforced concrete members by ultrasonic testing," *Cem. Concr. Res.*, Vol. 28, No. 7, 1071–1083, 1998.
6. Patil, S., B. Karkare, and S. Goyal, "Acoustic emission vis-a-vis electrochemical techniques for corrosion monitoring of reinforced concrete element," *Constr. Build. Mater.*, Vol. 68, 326–332, 2014.
7. Zaki, A., H. K. Chai, D. G. Aggelis, and N. Alver, "Non-destructive evaluation for corrosion monitoring in concrete: A review and capability of acoustic emission technique," *Sensors*, Vol. 15, No. 8, 19069–19101, 2015.
8. Ohtsu, M., K. Mori, and Y. Kawasaki, "Corrosion process and mechanisms of corrosion-induced cracks in reinforced concrete identified by AE analysis," *Strain*, Vol. 47, 179–186, 2011.
9. Xu, C., N. Zhou, J. Xie, X. Gong, G. Chen, and G. Song, "Investigation on eddy current pulsed thermography to detect hidden cracks on corroded metal surface," *NDT E Int.*, Vol. 84, 27–35, 2016.
10. Cacciola, M., S. Calcagno, G. Megali, F. C. Morabito, D. Pellicano, and M. Versaci, "FEA design and misfit minimization for in-depth flaw characterization in metallic plates with eddy current nondestructive testing," *IEEE Trans. Magn.*, Vol. 45, No. 3, 1506–1509, 2009.
11. Buonsanti, M., M. Cacciola, G. Megali, F. C. Morabito, D. Pellicanò, and M. Versaci, "A rotating magnetic field for detection of cracks in metal welded joints and quality control," *Proceedings of the Ninth International Conference on Computational Structures Technology*, Paper 68, Stirlingshire, UK, 2008.
12. Kylili, A., P. A. Fokaides, P. Christou, and S. A. Kalogirou, "Infrared thermography (IRT) applications for building diagnostics: A review," *Appl. Energy*, Vol. 134, 531–549, 2014.
13. Bagavathiappan, S., B. B. Lahiri, T. Saravanan, J. Philip, and T. Jayakumar, "Infrared thermography for condition monitoring — A review," *Infrared Phys. Technol.*, Vol. 60, 35–55, 2013.
14. Kobayashi, K. and N. Banthia, "Corrosion detection in reinforced concrete using induction heating and infrared thermography," *J. Civ. Struct. Health Monit.*, Vol. 1, No. 1–2, 25–35, 2011.
15. Hong, S., H. Wiggenhauser, R. Helmerich, B. Dong, P. Dong, and F. Xing, "Long-term monitoring of reinforcement corrosion in concrete using ground penetrating radar," *Corros. Sci.*, Vol. 114, 123–132, 2017.
16. Zhang, H., L. Liao, R. Zhao, J. Zhou, M. Yang, and R. Xia, "The non-destructive test of steel corrosion in reinforced concrete bridges using a micro-magnetic sensor," *Sensors*, Vol. 16, No. 9, 1439, 2016.
17. Fernandes, B., D. Nims, and V. Devabhaktuni, "Comprehensive MMF-MFL inspection for corrosion detection and estimation in embedded prestressing strands," *J. Civ. Struct. Health Monit.*, Vol. 4, No. 1, 43–55, 2014.
18. Xu, Y., K. Li, L. Liu, L. Yang, X. Wang, and Y. Huang, "Experimental study on rebar corrosion using the galvanic sensor combined with the electronic resistance technique," *Sensors*, Vol. 16, No. 9, 1451, 2016.
19. Tan, C. H., Y. G. Shee, B. K. Yap, and F. R. M. Adikan, "Fiber Bragg grating based sensing system: Early corrosion detection for structural health monitoring," *Sens. Actuators Phys.*, Vol. 246, 123–128, 2016.
20. Mao, J., J. Chen, L. Cui, W. Jin, C. Xu, and Y. He, "Monitoring the corrosion process of reinforced concrete using BOTDA and FBG sensors," *Sensors*, Vol. 15, No. 4, 8866–8883, 2015.
21. Takahashi, Y., "In-situ X-ray diffraction of corrosion products formed on iron surfaces," *Mater. Trans.*, Vol. 46, No. 3, 637–642, 2005.
22. Wu, Z., "Imaging of soft material with carbon nanotube tip using near-field scanning microwave microscopy," *Ultramicroscopy*, Vol. 148, 75–80, 2015.

23. Kawata, S., Y. Inouye, and P. Verma, "Plasmonics for near-field nano-imaging and superlensing," *Nat. Photonics*, Vol. 3, No. 7, 388–394, 2009.
24. Oka, S., H. Togo, N. Kukutsu, and T. Nagatsuma, "Latest trends in millimeter-wave imaging technology," *Progress In Electromagnetics Research Letters*, Vol. 1, 197–204, 2008.
25. Balanis, C. A., *Antenna Theory: Analysis and Design*, John Wiley & Sons, 2015.
26. Wang, P., Y. Pei, and L. Zhou, "Near-field microwave identification and quantitative evaluation of liquid ingress in honeycomb sandwich structures," *NDT E Int.*, Vol. 83, 32–37, 2016.
27. Haddadi, K., S. Gu, and T. Lasri, "Sensing of liquid droplets with a scanning near-field microwave microscope," *Sens. Actuators Phys.*, Vol. 230, 170–174, 2015.
28. Hussein, K. F. A., "Efficient near-field computation for radiation and scattering from conducting surfaces of arbitrary shape," *Progress In Electromagnetics Research*, Vol. 69, 267–285, 2007.
29. Haddadi, K., J. Marzouk, S. Gu, S. Arscott, G. Dambrine, and T. Lasri, "Interferometric near-field microwave microscopy platform for electromagnetic micro-analysis," *Procedia Eng.*, Vol. 87, 388–391, 2014.
30. Esslinger, M. and R. Vogelgesang, "Reciprocity theory of apertureless scanning near-field optical microscopy with point-dipole probes," *Acs Nano*, Vol. 6, No. 9, 8173–8182, 2012.
31. Sundaramurthy, A., P. J. Schuck, N. R. Conley, D. P. Fromm, G. S. Kino, and W. E. Moerner, "Toward nanometer-scale optical photolithography: Utilizing the near-field of bowtie optical nanoantennas," *Nano Lett.*, Vol. 6, No. 3, 355–360, 2006.
32. Gao, C., X. Xiang, and Z. Wu, "Novel scanning tip microwave near-field microscopy," *Physics*, Vol. 68, No. 68, 3506–3508, 1999.
33. Castro, A. F., M. Valcuende, and B. Vidal, "Using microwave near-field reflection measurements as a non-destructive test to determine water penetration depth of concrete," *NDT E Int.*, Vol. 75, 26–32, 2015.